ELSEVIER

Journal of Organometallic Chemistry 662 (2002) 105–111

Journal of Organometallic Chemistry

www.elsevier.com/locate/jorganchem

On the transferability of Ir–I bond enthalpies between [Ir(μ-S^{t}Bu)(I)$_2$(CO)$_2$]$_2$ and *trans*-[Ir(X)(I)$_2$(CO)(PPh$_3$)$_2$] (X = F, Cl, Br, I) complexes

Luís F. Veiros, Manuel E. Minas da Piedade *

Centro de Química Estrutural, Complexo Interdisciplinar, Instituto Superior Técnico, 1049-001 Lisboa, Portugal

Received 5 July 2002; accepted 11 August 2002

Abstract

The transferability of the Ir–I bond enthalpies in [Ir(μ-S^{t}Bu)(I)$_2$(CO)$_2$]$_2$ and *trans*-[Ir(X)(I)$_2$(CO)(PPh$_3$)$_2$] (X = F, Cl, Br, I) complexes was investigated by theoretical calculations based on the B3LYP HF/DFT hybrid functional. It was concluded that the Ir–I bond snap enthalpy, E_s(Ir–I), in [Ir(μ-S^{t}Bu)(I)$_2$(CO)$_2$]$_2$ was 35 kJ mol^{-1} smaller than in *trans*-[Ir(X)(I)$_2$(CO)(PPh$_3$)$_2$] and, therefore, not transferable between both types of molecules. The relative magnitude of the obtained E_s(Ir–I) values is in agreement with the slightly longer Ir–I distance and smaller Wiberg index found, on average, for [Ir(μ-S^{t}Bu)(I)$_2$(CO)$_2$]$_2$. In this case, however, the computed d_{Ir-I} and WI_{Ir-I} do not seem to be sensitive indicators of 'bond strength', since a variation of 35 kJ mol^{-1} in the E_s(Ir–I) values leads to changes of only 0.01 Å in the bond distances and 0.005 in the Wiberg indexes. The calculations reproduce the experimental Ir–I mean bond dissociation enthalpies, $\langle DH^\circ \rangle$(Ir–I), in the binuclear and mononuclear systems with a maximum deviation of ca. 10 kJ mol^{-1}.

Keywords: Bond dissociation enthalpy; Thermochemistry; Density functional theory; Iridium complexes

1. Introduction

In a previous study on the energetics of the *trans*-annular oxidative addition of I$_2$ to [Ir(μ-S^{t}Bu)(CO)$_2$]$_2$ we observed that the Ir–I mean bond dissociation enthalpy in solution in the complex [Ir(μ-S^{t}Bu)(I)$_2$(CO)$_2$]$_2$, $\langle DH^\circ \rangle$(Ir–I) in Eq. (1), was significantly smaller (ca. 9–40 kJ mol^{-1}, with a mean value of 26.0 ± 2.5 kJ mol^{-1} [1–4]) than the corresponding values in a variety of mononuclear complexes *trans*-[Ir(X)(I)$_2$(CO)(L)$_2$] (Eq. (2); L = PPh$_3$, X = F, Cl, Br, I, NCS, N$_3$, CS; X = Cl, L = PPhMe$_2$, PPhEt$_2$, PPh$_2$Me, PPh$_2^t$Bu, PCy$_3$, P(OPh)$_3$, AsPh$_3$; Me = CH$_3$, Et = C$_2$H$_5$, ^{t}Bu = ^{t}C$_4$H$_9$, Ph = C$_6$H$_5$, Cy = C$_6$H$_{11}$).

$$[Ir(\mu\text{-}S^tBu)(I)_2(CO)_2]_2(sln) \xrightarrow{\langle DH^\circ \rangle(Ir-I)} [Ir(\mu\text{-}S^tBu)(CO)_2]_2(sln) + 4I(sln) \quad (1)$$

$$trans\text{-}[Ir(X)(I)_2(CO)(L)_2](sln) \xrightarrow{\langle DH^\circ \rangle(Ir-I)} trans\text{-}[Ir(X)(CO)(L)_2](sln) + 2I(sln) \quad (2)$$

The contrast with the *trans*-[Ir(X)(I)$_2$(CO)(PPh$_3$)$_2$] (X = F, Cl, Br, I) derivatives seemed particularly interesting. In fact, extended Hückel molecular orbital calculations on the model systems [Ir(μ-SMe)(I)$_2$(CO)$_2$]$_2$ and *trans*-[Ir(X)(I)$_2$(CO)(PH$_3$)$_2$] (X = F, Cl, Br and I) predicted Ir–I overlap populations of 0.40 in the binuclear and 0.39 in each of the four mononuclear complexes. Since the overlap population (OP) is a widely used indicator of 'bond strength' [5], this suggested that, although in [Ir(μ-S^{t}Bu)(I)$_2$(CO)$_2$]$_2$ $\langle DH^\circ \rangle$ (Ir–I) = 122.2 ± 0.7 kJ mol^{-1} [1] and in *trans*-[Ir(X)(I)$_2$(CO)(PPh$_3$)$_2$] $\langle DH^\circ \rangle$ (Ir–I) = 149.0 ± 6.7 (X = F) [2,4], 143.8 ± 2.5 (X = Cl) [2,4], 151.0 ± 0.8 (X = Cl) [3,4], 149.8 ± 2.1 (X = Br) [2,4], and 135.6 ± 5.0 kJ mol^{-1} (X = I) [2,4], no relevant 'bond strength' difference was to be expected between the Ir–I bonds in the binuclear and mononuclear complexes [1].

The OP is more likely to correlate with metal–ligand *bond snap enthalpies*, E_s(M–L), than with *bond dissocia-*

* Corresponding author

E-mail address: pcmemp@popsrv.ist.utl.pt (M.E. Minas da Piedade).

0022-328X/02/$ - see front matter © 2002 Elsevier Science B.V. All rights reserved.
PII: S0022-328X(02)01896-X

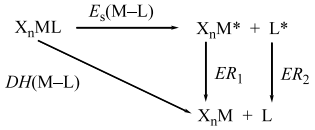

Scheme 1.

tion enthalpies, DH(M–L) [6]. This can be understood by considering Scheme 1, which shows the relation between these two thermochemical measures of 'bond strength' for a hypothetical X_nML complex (M = transition metal; X, L = ligands). Here the asterisks designate fragments retaining the geometry of the precursor complex and $ER_1$and ER_2 are the *reorganisation energies* associated with the relaxation of X_nM^* and L* to originate X_nM and L in their ground states, respectively.

Scheme 1 directly leads to Eq. (3):

$$DH(\text{M–L}) = E_s(\text{M–L}) + ER_1 + ER_2 \quad (3)$$

The E_s(M–L) values do not contain the reorganisation energies and are therefore expected to correlate better with structural data, such as overlap populations or bond lengths, than DH(M–L). This led us to speculate that E_s(Ir–I) might be approximately constant in [Ir(μ-S^{t}Bu)(I)$_2$(CO)$_2$]$_2$ and in *trans*-[Ir(X)(I)$_2$(CO)(PPh$_3$)$_2$], and that the smaller $\langle DH^\circ\rangle$(Ir–I) observed in the binuclear complex reflected a more negative reorganisation energy of [Ir(μ-S^{t}Bu)(CO)$_2$]$_2^*$ when compared with [Ir(X)(CO)(PPh$_3$)$_2$]* [1]. This hypothesis could not, however, be tested, due to the impossibility of computing the necessary ER data using reasonably accurate theoretical calculations. The problem is now addressed using ab initio [7] and density functional theory (DFT) [8] calculations.

2. Computational details

The geometry optimisations and energy computations were accomplished by means of ab initio and DFT calculations performed with the GAUSSIAN-98 program [9], using the B3LYP hybrid functional. This functional comprises a mixture of Hartree-Fock [7] exchange with DFT [8] exchange-correlation, given by Becke's three parameter functional [10] with the Lee, Yang and Parr correlation functional, which includes both local and non-local terms [11,12]. All reported geometries are the result of full optimisations without any symmetry constraints. The S^{t}Bu groups on the binuclear species and the PPh$_3$ ligands on the mononuclear complexes were modelled by SMe and PH$_3$, respectively. A valence double zeta with polarisation (DZP) basis set was used for the geometry optimisations, namely, a standard LanL2DZ [13,14] basis set with an f-polarisation function added for Ir [15] and a d-polarisation function for I and Br [16]; the other elements were described by a standard D95* basis set [13]. All stationary points were confirmed as minima by means of vibration frequency calculations. Single point energy calculations were performed on the optimised structures of [Ir(μ-SMe)(I)$_2$(CO)$_2$]$_2$, [Ir(μ-SMe)(CO)$_2$]$_2$, *trans*-[Ir(X)(I)$_2$(CO)(PH$_3$)$_2$], and [Ir(X)(CO)(PH$_3$)$_2$] (X = Cl, Br), with the same functional and a valence triple zeta with polarisation (TZP) basis set, that consisted of a standard 6-311G** [17] for all the atoms, except Ir and I; in these cases the Stuttgart/Dresden effective core potentials with triple zeta valence (SDD) [18] was used, with an f- and a d-polarisation function added for Ir and I, respectively. The obtained energies were converted to standard enthalpies at 298.15 K by using zero point energy and thermal energy corrections based on structural and vibration frequency data calculated at the B3LYP/DZP level of theory. The reorganisation energies of the [Ir(μ-SMe)(I)$_2$(CO)$_2$]$_2^*$ and [Ir(X)(CO)(PH$_3$)$_2$]* species were obtained from single point energy calculations (B3LYP/TZP) on the geometries of the non-reorganised and reorganised fragments without zero point or thermal energy corrections. A natural population analysis (NPA) [19] was performed, in order to obtain the Wiberg indexes [20] used to evaluate the Ir–I 'bond strength'. The calculated vibrational frequencies reported in Section 3 were scaled by a 0.9613 factor [21], but the zero point and thermal energy corrections mentioned above were derived without scaling.

3. Results and discussion

It can be concluded from Scheme 2 that the constancy of E_s(Ir–I) in [Ir(μ-S^{t}Bu)(I)$_2$(CO)$_2$]$_2$ and *trans*-[Ir(X)(I)$_2$(CO)(PPh$_3$)$_2$] complexes directly leads to Eq. (4):

$$\langle DH^\circ\rangle(\text{Ir–I}) = \langle DH^\circ\rangle(\text{Ir–I})' + \frac{ER_1}{4} - \frac{ER_2}{2} \quad (4)$$

where $\langle DH^\circ\rangle$(Ir–I) and $\langle DH^\circ\rangle$(Ir–I)′ represent the Ir–I mean bond dissociation enthalpies in solution for the complexes [Ir(μ-S^{t}Bu)(I)$_2$(CO)$_2$]$_2$ and *trans*-

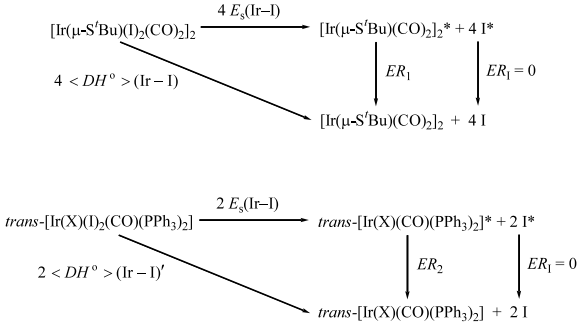

Scheme 2.

$[Ir(X)(I)_2(CO)(PPh_3)_2]$, and ER_1 and ER_2 are the reorganisation energies of the corresponding $[Ir(\mu\text{-}S^tBu)(CO)_2]_2^*$ and $[Ir(X)(CO)(PPh_3)_2]^*$ fragments. According to this equation, as the reorganisation energies have negative values, the fact that $\langle DH^\circ\rangle$(Ir–I) is smaller than $\langle DH^\circ\rangle$(Ir–I)′ implies that $|ER_1/4| > |ER_2/2|$. The ER values are not experimentally accessible but can be predicted through quantum chemistry calculations. In this case B3LYP (HF/DFT) calculations were used to obtain $\langle DH^\circ\rangle$(Ir–I), $\langle DH^\circ\rangle$(Ir–I)′, ER_1 and ER_2, and test the transferability of E_s(Ir–I) between $[Ir(\mu\text{-}S^tBu)(I)_2(CO)_2]_2$ and *trans*-$[Ir(X)(I)_2(CO)(PPh_3)_2]$ complexes.

The first step of the computational analysis of Scheme 2 was, however, the geometry optimisation of $[Ir(\mu\text{-}SMe)(I)_2(CO)_2]_2$, $[Ir(\mu\text{-}SMe)(CO)_2]_2$, *trans*-$[Ir(X)(I)_2(CO)(PH_3)_2]$, and $[Ir(X)(CO)(PH_3)_2]$ (X = Cl, Br). Since the molecular structures of these model systems and of the original complexes in Scheme 2 have not been experimentally determined, the reliability of the calculations was assessed by comparing the optimised geometry of $[Ir(\mu\text{-}SMe)I(CO)_2]_2$ with that of $[Ir(\mu\text{-}S^tBu)I(CO)_2]_2$ obtained by X-ray diffraction [1] (Fig. 1). As shown in Fig. 1, a very good general agreement is observed between the model and experimental structures. Both molecules can be viewed as composed by two square pyramidal Ir^{II} fragments, $[Ir(\mu\text{-}SR)_2(CO)_2I]$ (R = Me, ^{t}Bu), sharing one S–S edge. In each fragment the iodine occupies the axial position, and the two CO ligands and the two sulphur bridges define the equatorial plane. The geometry of the complex core (i.e. Ir–S–Ir–S ring) is well reproduced by the calculations, despite the use of SMe groups to model the S^{t}Bu bridges that are present in the original complex. Both the calculated and experimental structures exhibit a relatively narrow angle (93°) between the equatorial planes of the two square pyramidal fragments in order to allow an Ir–Ir interaction that provides the 18-electron count on each metal (the Ir–Ir Wiberg index is 0.222). The Ir–Ir distances are 2.64 and 2.72 Å in the experimental and optimised structures, respectively.

A more extended comparison between the geometrical features of both molecules in Fig. 1 confirms the reliability of the theoretical model. In fact the Ir–X, C–O and S–C bond distances in the model structure show mean and maximum absolute deviations of 0.053 and 0.096 Å, respectively, from the corresponding distances in the experimental structure. All the calculated distances are slightly larger than the experimental ones, with the exception of the S–C bond lengths, which show the opposite trend: 1.836 and 1.838 Å (calculated), and 1.880 and 1.908 Å (experimental).

The optimised geometries of $[Ir(\mu\text{-}SMe)(I)_2(CO)_2]_2$, and $[Ir(\mu\text{-}SMe)(CO)_2]_2$, which model the binuclear molecules in Scheme 2, are shown in Fig. 2. The $[Ir(\mu\text{-}SMe)(I)_2(CO)_2]_2$ complex can be viewed as being formed

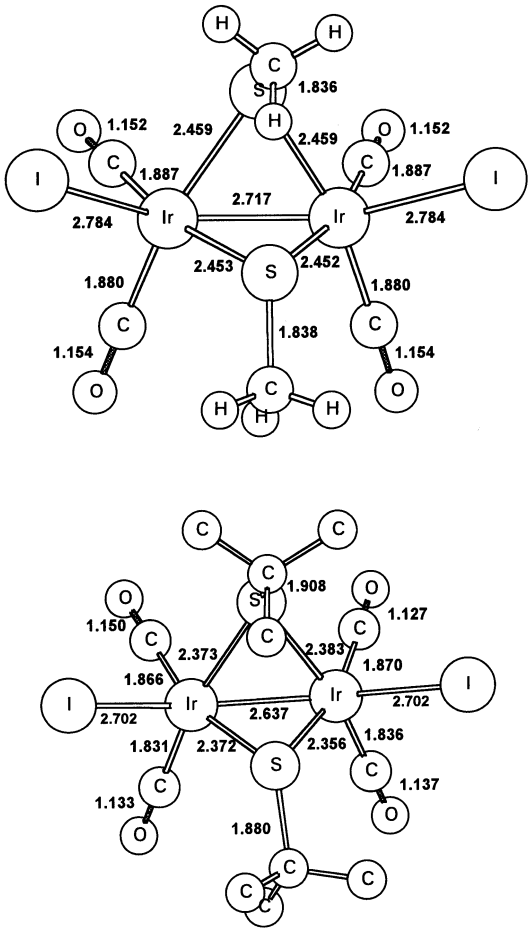

Fig. 1. Optimised geometry (B3LYP/DZP) of $[Ir(\mu\text{-}SMe)I(CO)_2]_2$ (top) and X-ray structure of $[Ir(\mu\text{-}S^tBu)I(CO)_2]_2$ [1] (bottom; hydrogens omitted for clarity). The more relevant bond distances (Å) are shown.

by two $[Ir(\mu\text{-}SMe)_2(I)_2(CO)_2]$ moieties, each exhibiting an approximately octahedral environment around the Ir^{III} centre, as expected for a d^6 metal and a 18-electron species. The two iodine atoms occupy the axial positions, and the equatorial plane is defined by the two carbonyl groups and by the two sulphur bridges. The angle between the equatorial planes of both moieties is 180°. The long Ir–Ir distance (3.77 Å) indicates the absence of any significant metal–metal bonding, as expected on the basis of simple electron counting rules (see above) and confirmed by the Wiberg index (0.082). Despite the absence of symmetry constraints on the calculations (see Section 2) a highly symmetrical structure (C_{2h}) was obtained with equivalent bond distances identical within 0.001 Å. Moderate distortions from a regular octahedral geometry are, nevertheless, found around each Ir centre. The bond angles in the equatorial plane (C–Ir–C = 95, and S–Ir–S = 81°) deviate from 90° as a result of the geometrical constraints imposed on the Ir–S–Ir–S ring by the sulphur bridges. Furthermore the obtained I–Ir–I angle (171°) is smaller than 180°,

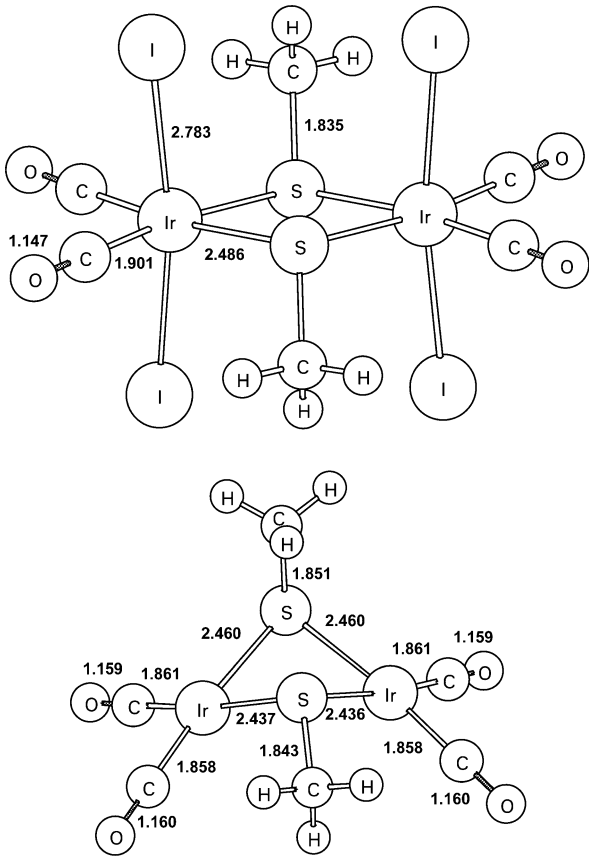

Fig. 2. Optimised geometries (B3LYP/DZP) of the binuclear complexes $[Ir(\mu\text{-}SMe)(I)_2(CO)_2]_2$ (top) and $[Ir(\mu\text{-}SMe)(CO)_2]_2$ (bottom). The more relevant bond distances (Å) are presented.

showing that the iodine ligands are slightly bent in order to minimise the steric repulsion with the methyl groups on the bridging thiolates.

In the $[Ir(\mu\text{-}SMe)(CO)_2]_2$ complex each Ir^I centre adopts the square planar coordination environment typical of d^8 metals. The angle between the planes of the two $[Ir(\mu\text{-}SMe)_2(CO)_2]$ fragments is 121°, showing that in the absence of the steric constraints imposed by axial iodine ligands, it is the pyramidal geometry around the bridging sulphur atoms that determines the overall structure of the molecule. The large Ir–Ir distance (3.36 Å) observed precludes the existence of a metal–metal bond, as further confirmed by the small Wiberg index value of 0.031. It is also interesting to note that, as expected, the higher electronic density on the Ir^I centres in $[Ir(\mu\text{-}SMe)(CO)_2]_2$ (the calculated Ir NPA [19] charge is −0.07) when compared with that of the Ir^{III} centres in $[Ir(\mu\text{-}SMe)_2(I)_2(CO)_2]$ (0.108 Ir NPA charge) leads to an increased Ir→CO backdonation in the former species. This is indicated by various results, namely: (i) the decrease of the Ir–C bond lengths (from 1.90 to 1.86 Å) and the increase of the C–O distances (from 1.15 to 1.16 Å) on going from the $(Ir^{III})_2$ to the $(Ir^I)_2$ complex; (ii) the change of the Wiberg index for the Ir–C bonds from 0.772 $(Ir^{III})_2$ to 1.010–1.026 $(Ir^I)_2$, and for the C–O bonds from 2.194 $(Ir^{III})_2$ to 2.102–2.112 $(Ir^I)_2$; and (iii) the decrease of computed C–O stretching frequencies from 2059–2098 $(Ir^{III})_2$ to 1987–2054 cm^{-1} $(Ir^I)_2$. An intermediate behaviour is found in the $(Ir^{II})_2$ complex discussed above (Fig. 1).

The optimised geometries of $[Ir(X)(I)_2(CO)(PH_3)_2]$ and $[Ir(X)(CO)(PH_3)_2]$ (X = Cl, Br), which model the mononuclear species in Scheme 2, are shown in Fig. 3. The $[Ir(X)(I)_2(CO)(PH_3)_2]$ complexes (Fig. 3 top) exhibit an octahedral geometry with small distortions around the Ir^{III} centre. The iodine ligands occupy the axial positions and the equatorial plane is defined by the carbonyl, by the halogen, and by the two phosphine ligands. The distortions are due to the asymmetry in the equatorial plane and consist, for example, in the observation of a I–Ir–I angle (174°) smaller than 180° and angles between the equatorial phosphines larger than 90° (97 and 96° for X = Cl and Br, respectively). Almost identical geometries were obtained for the chloride and the bromide complexes, with mean and maximum absolute differences between equivalent bond lengths of 0.002 and 0.006 Å, respectively.

The $[Ir(X)(CO)(PH_3)_2]$ complexes illustrated at the bottom of Fig. 3, have an approximately square planar geometry. The distortions around the Ir^I centre are caused by the same type of asymmetry present in the octahedral *trans*-$[Ir(X)(I)_2(CO)(PH_3)_2]$ species (see above) as shown by the larger than 90° P–Ir–P angle (96° for X = Cl and 95° for X = Br). As in the case of *trans*-$[Ir(X)(I)_2(CO)(PH_3)_2]$ the geometries of the chloride and bromide derivatives of $[Ir(X)(CO)(PH_3)_2]$ are practically identical with mean and maximum absolute differences between equivalent bond lengths of 0.002 and 0.003 Å, respectively.

It is important to stress the structural similarity between the mononuclear and binuclear complexes represented in Figs. 3 and 2, respectively. Not only with respect to the overall geometry (octahedral for the Ir^{III} centres and square planar for the Ir^I centres) but also in terms of the computed distances for equivalent bonds. Thus, for the octahedral species the Ir–C bond lengths are only 0.01 Å longer in $[Ir(\mu\text{-}SMe)(I)_2(CO)_2]_2$ than in *trans*-$[Ir(X)(I)_2(CO)(PH_3)_2]$; the C–O distances are identical within 0.002 Å in both molecules; and, although longer axial Ir–I bonds are observed in the binuclear than in the mononuclear complex, the maximum difference is 0.015 Å. The same analogy is found when comparing the Ir^I complexes, $[Ir(\mu\text{-}SMe)(CO)_2]_2$ and $[Ir(X)(CO)(PH_3)_2]$, which show equal Ir–C and C–O bond distances within 0.002 Å.

Single point enthalpy calculations at the B3LYP/DZP and B3LYP/TZP level of theory, on the optimised B3LYP/DZP geometries of $[Ir(\mu\text{-}SMe)(I)_2(CO)_2]_2$, $[Ir(\mu\text{-}SMe)(CO)_2]_2$, *trans*-$[Ir(X)(I)_2(CO)(PH_3)_2]$, and $[Ir(X)(CO)(PH_3)_2]$ (X = Cl, Br) discussed above, yielded the mean Ir–I bond dissociation enthalpies in Table 1,

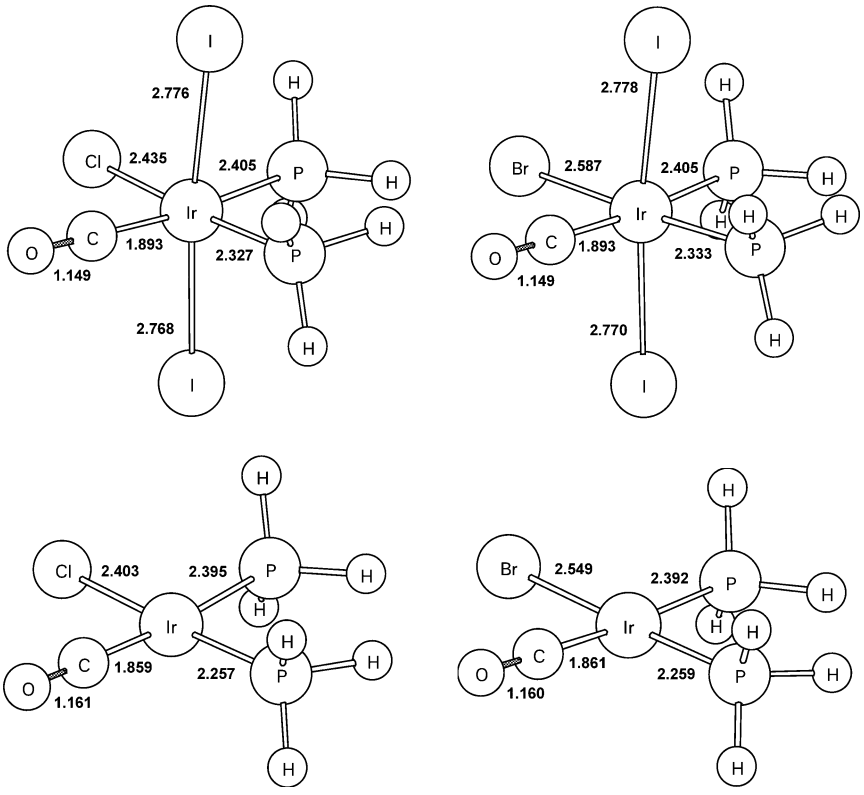

Fig. 3. Optimised geometries (B3LYP/DZP) of the mononuclear complexes *trans*-[Ir(X)(I)$_2$(CO)(PH$_3$)$_2$] (top), and [Ir(X)(CO)(PH$_3$)$_2$] (bottom). The chloride derivatives (X = Cl) are shown on the left side and the bromide derivatives (X = Br) on the right side. The more relevant bond distances (Å) are presented.

which correspond to the reactions in Scheme 2. As seen in Table 1, the results are quite insensitive to the basis set used in the calculation. The agreement between the $\langle DH^\circ\rangle$(Ir–I) values computed for the model systems and the corresponding experimental values reported for *trans*-[Ir(X)(I)$_2$(CO)(PPh$_3$)$_2$] and [Ir(μ-S^{t}Bu)(I)$_2$(CO)$_2$]$_2$, in solution, can be considered excellent, given that the accuracy normally claimed for experimental bond dissociation enthalpy data of organometallic systems is seldom better than 5–10 kJ mol^{-1} [22–29]. Hence, in agreement with experimental observations, the results of the calculations also indicate that $\langle DH^\circ\rangle$(Ir–I) is smaller in the binuclear complexes than in the mononuclear complexes.

Also listed in Table 1 are the reorganisation energies of the [Ir(μ-SMe)(CO)$_2$]$_2^*$ and [Ir(X)(CO)(PH$_3$)$_2$]* fragments (Scheme 2). The ER values were obtained from single point energy calculations (B3LYP/TZP) on the

Table 1
Ir–I mean bond dissociation enthalpies, $\langle DH^\circ\rangle$(Ir–I), bond snap enthalpies, E_s(Ir–I), reorganisation energies, ER, bond distances, d_{Ir-I}, and Wiberg indexes, WI_{Ir-I}

Complex	$\langle DH^\circ\rangle$(Ir–I) (kJ mol^{-1})	E_s(Ir–I) (kJ mol^{-1}) [a]	ER (kJ mol^{-1}) [c]	$\langle d_{Ir-I}\rangle$/Å	$\langle WI_{Ir-I}\rangle$
[Ir(μ-SMe)(I)$_2$(CO)$_2$]$_2$	125 [a]; 119 [b]	120	22	2.783	0.465
[Ir(μ-S^{t}Bu)(I)$_2$(CO)$_2$]$_2$	122.2 ± 0.7 [1] [d]				
trans-[Ir(X)(I)$_2$(CO)(PH$_3$)$_2$]					
X = Cl	159 [a]; 155 [b]	155	8	2.772	0.470
X = Br	158 [a]; 154 [b]	155	7	2.774	0.470
trans-[Ir(X)(I)$_2$(CO)(PPh$_3$)$_2$]					
X = Cl	143.8 ± 2.5 [2,4] [d]				
	151.0 ± 0.8 [3,4] [d]				
X = Br	149.8 ± 2.1 [2,4] [d]				

[a] B3LYP/TZP//B3LYP/DZP including zero point energy and thermal corrections calculated at the B3LYP/DZP level of theory.
[b] B3LYP/DZP including zero point energy and thermal corrections.
[c] B3LYP/TZP//B3LYP/DZP, see text.
[d] Experimental.

geometries of the non-reorganised and reorganised fragments obtained at the B3LYP/DZP level of theory without zero point or thermal energy corrections (see Section 2). It was assumed that the $[Ir(\mu\text{-}SMe)(CO)_2]_2^*$ and $[Ir(X)(CO)(PH_3)_2]^*$ fragments retained the same structure they had in the precursor complexes.

The calculated $\langle DH^\circ \rangle$(Ir–I) and ER data led to the E_s(Ir–I) values in Table 1 through Eq. (3) where, in keeping with Scheme 2, $ER_I = 0$ was assumed. The obtained results indicate that the Ir–I bond snap enthalpies are not transferable between the $[Ir(\mu\text{-}S^tBu)(I)_2(CO)_2]_2$ and *trans*-$[Ir(X)(I)_2(CO)(PPh_3)_2]$, since they differ by 35 kJ mol^{-1}. The fact that E_s(Ir–I) is smaller in $[Ir(\mu\text{-}S^tBu)(I)_2(CO)_2]_2$ than in *trans*-$[Ir(X)(I)_2(CO)(PPh_3)_2]$ is in agreement with the slightly longer Ir–I distance and smaller Wiberg index computed on average for the binuclear complex, when compared with the mononuclear complexes (Table 1). In this case, however, the computed d_{Ir-I} and WI_{Ir-I} do not seem to be sensitive indicators of 'bond strength', since a variation of 35 kJ mol^{-1} in the E_s(Ir–I) values leads to changes of only 0.01 Å in the bond distances and 0.005 in the Wiberg indexes (Table 1).

Acknowledgements

This work was supported by Fundação para a Ciência e a Tecnologia, Portugal (Project POCTI/199/QUI/35406).

References

[1] M.A. Ciriano, A.R. Dias, P.M. Nunes, L.A. Oro, M.F. Minas da Piedade, M.E. Minas da Piedade, P. Ferreira da Silva, J.A. Martinho Simões, J.J. Pérez-Torrente, L.F. Veiros, Struct. Chem. 7 (1996) 337.
[2] N.E. Burke, A. Singhal, M.J. Hintz, J.A. Ley, H. Hui, L.R. Smith, D.M. Blake, J. Am. Chem. Soc. 101 (1979) 74.
[3] R.S. Drago, M.S. Nozari, R.J. Klinger, C.S. Chamberlain, Inorg. Chem. 18 (1979) 1254.
[4] J.A. Martinho Simões, Organometallic thermochemistry data, in: W.G. Mallard, P.J. Linstrom (Eds.), NIST Chemistry WebBook, NIST Standard Reference Database Number 69, National Institute of Standards and Technology, Gaithersburg, February 2000, (http://webbook.nist.gov/chemistry).
[5] J.K. Burdett, Molecular Shapes, John Wiley, New York, 1980, p. 14.
[6] J.A. Martinho Simões, in: J.A. Martinho Simões (Ed.), Energetics of Organometallic Species, NATO ASI Ser., Ser. C, vol. 367, Kluwer, Dordrecht, 1992, p. 197.
[7] W.J. Hehre, L. Radom, P.v.R. Schleyer, J.A. Pople, Ab Initio Molecular Orbital Theory, John Wiley, New York, 1986.
[8] R.G. Parr, W. Yang, Density Functional Theory of Atoms and Molecules, Oxford University Press, New York, 1989.
[9] M.J. Frisch, G.W. Trucks, H.B. Schlegel, G.E. Scuseria, M.A. Rob, J.R. Cheeseman, V.G. Zakrzewski, J.A. Montgomery, Jr., R.E. Stratmann, J.C. Burant, S. Dapprich, J.M. Millam, A.D. Daniels, K.N. Kudin, M.C. Strain, O. Farkas, J. Tomasi, V. Barone, M. Cossi, R. Cammi, B. Mennucci, C. Pomelli, C. Adamo, S. Clifford, J. Ochterski, G.A. Petersson, P.Y. Ayala, Q. Cui, K. Morokuma, D.K. Malick, A.D. Rabuck, K. Raghavachari, J.B. Foresman, J. Cioslowski, J.V. Ortiz, A.G. Baboul, B.B. Stefanov, G. Liu, A. Liashenko, P. Piskorz, I. Komaromi, R. Gomperts, R.L. Martin, D.J. Fox, T. Keith, M.A. Al-Laham, C.Y. Peng, A. Nanayakkara, C. Gonzalez, M. Challacombe, P.M.W. Gill, B. Johnson, W. Chen, M.W. Wong, J.L. Andres, C. Gonzalez, M. Head-Gordon, E.S. Replogle, and J.A. Pople, GAUSSIAN-98, Revision A.7, Gaussian, Inc., Pittsburgh, 1998.
[10] A.D. Becke, Chem. Phys. 98 (1993) 5648.
[11] C. Lee, W. Yang, R.G. Parr, Phys. Rev. B 37 (1988) 785.
[12] B. Miehlich, A. Savin, H. Stoll, H. Preuss, Chem. Phys. Lett. 157 (1989) 200.
[13] T.H. Dunning, Jr., P.J. Hay, in: H.F. Schaefer (Ed.), Modern Theoretical Chemistry, vol. 3, Plenum, New York, 1976, p. 1.
[14] (a) P.J. Hay, W.R. Wadt, J. Chem. Phys. 82 (1985) 270;
(b) W.R. Wadt, P.J. Hay, J. Chem. Phys. 82 (1985) 284;
(c) P.J. Hay, W.R. Wadt, J. Chem. Phys. 82 (1985) 2299.
[15] A.W. Ehlers, M. Böhme, S. Dapprich, A. Gobbi, A. Höllwarth, V. Jonas, K.F. Köhler, R. Stegmann, A. Veldkamp, G. Frenking, Chem. Phys. Lett. 208 (1993) 111.
[16] A. Höllwarth, M. Böhme, S. Dapprich, A.W. Ehlers, A. Gobbi, V. Jonas, K.F. Köhler, R. Stegmann, A. Veldkamp, G. Frenking, Chem. Phys. Lett. 208 (1993) 237.
[17] (a) A.D. McClean, G.S. Chandler, J. Chem. Phys. 72 (1980) 5639;
(b) R. Krishnan, J.S. Binkley, R. Seeger, J.A. Pople, J. Chem. Phys. 72 (1980) 650;
(c) A.J.H. Wachters, J. Chem. Phys. 52 (1970) 1033;
(d) P.J. Hay, J. Chem. Phys. 66 (1977) 4377;
(e) K. Raghavachari, G.W. Trucks, J. Chem. Phys. 91 (1989) 1062;
(f) R.C. Binning, L.A. Curtiss, J. Comput. Chem. 103 (1995) 6104;
(g) M.P. McGrath, L. Radom, J. Chem. Phys. 94 (1991) 511.
[18] (a) U. Haeusermann, M. Dolg, H. Stoll, H. Preuss, Mol. Phys. 78 (1993) 1211;
(b) W. Kuechle, M. Dolg, H. Stoll, H. Preuss, J. Chem. Phys. 100 (1994) 7535;
(c) T. Leininger, A. Nicklass, H. Stoll, M. Dolg, P. Schwerdtfeger, J. Chem. Phys. 105 (1996) 1052.
[19] (a) J.E. Carpenter, F. Weinhold, J. Mol. Struct. (Theochem) 169 (1988) 41;
(b) J.E. Carpenter, PhD thesis, University of Wisconsin, Madison, WI, 1987;
(c) J.P. Foster, F. Weinhold, J. Am. Chem. Soc. 102 (1980) 7211;
(d) A.E. Reed, F. Weinhold, J. Chem. Phys. 78 (1983) 4066;
(e) A.E. Reed, F. Weinhold, J. Chem. Phys. 78 (1983) 1736;
(f) A.E. Reed, R.B. Weinstock, F. Weinhold, J. Chem. Phys. 83 (1985) 735;
(g) A.E. Reed, L.A. Curtiss, F. Weinhold, Chem. Rev. 88 (1988) 899;
(h) F. Weinhold, J.E. Carpenter, The Structure of Small Molecules and Ions, Plenum, New York, 1988, p. 227.
[20] K.B. Wiberg, Tetrahedron 24 (1968) 1083.
[21] J.B. Foresman, Æ. Frisch, Exploring Chemistry with Electronic Structure Methods, 2nd ed., Gaussian Inc., Pittsburgh, 1996.
[22] Metal–Ligand Bonding Energetics in Organotransition Metal Compounds, T.J. Marks (Ed.), Polyhedron Symposium-in-Print, 7 (1988).
[23] Bonding Energetics in Organometallic Compounds, T.J. Marks (Ed.), ACS Symposium Series 428, American Chemical Society, Washington, 1990.
[24] J.A. Martinho Simões, J.L. Beauchamp, Chem. Rev. 90 (1990) 629.

[25] Energetics of Organometallic Species, J.A. Martinho Simões (Ed.), NATO ASI Ser., Ser. C, vol. 367, Kluwer, Dordrecht, 1992.
[26] C.D. Hoff, Prog. Inorg. Chem. 40 (1992) 503.
[27] P.B. Dias, M.E. Minas da Piedade, J.A. Martinho Simões, Coord. Chem. Rev. 135/136 (1994) 737.
[28] S.P. Nolan, Bonding energetics of organometallic compounds, in: R.B. King, Editor in Chief, Encyclopedia of Inorganic Chemistry, John Wiley, New York, 1994, p. 307.
[29] I.B. Rabinovich, V.P. Nistratov, V.I. Tel'noi, M.S. Sheiman, Thermochemical and Thermodynamic Properties of Organometallic Compounds, Begell House, New York, 1999.